

# Phosphonofluoresceins: Synthesis, Spectroscopy, and Applications

Joshua L. Turnbull, Brittany R. Benlian, Ryan P. Golden, and Evan W. Miller\*



Cite This: *J. Am. Chem. Soc.* 2021, 143, 6194–6201



Read Online

ACCESS |

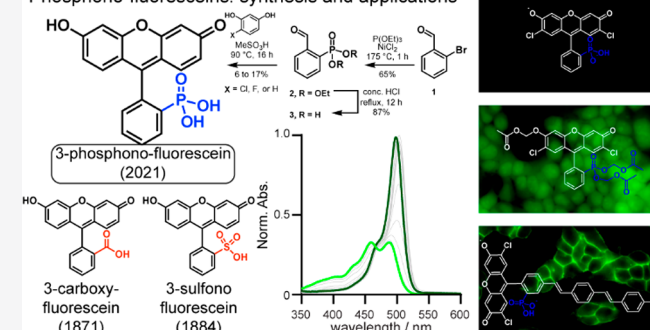
Metrics & More

Article Recommendations

Supporting Information

**ABSTRACT:** Xanthene fluorophores, like fluorescein, have been versatile molecules across diverse fields of chemistry and life sciences. Despite the ubiquity of 3-carboxy and 3-sulfonofluorescein for the last 150 years, to date, no reports of 3-phosphonofluorescein exist. Here, we report the synthesis, spectroscopic characterization, and applications of 3-phosphonofluoresceins. The absorption and emission of 3-phosphonofluoresceins remain relatively unaltered from the parent 3-carboxyfluorescein. 3-Phosphonofluoresceins show enhanced water solubility compared to 3-carboxyfluorescein and persist in an open, visible light-absorbing state even at low pH and in low dielectric media while 3-carboxyfluoresceins tend to lactonize. In contrast, the spirocyclization tendency of 3-phosphonofluoresceins can be modulated by esterification of the phosphonic acid. The bis-acetoxymethyl ester of 3-phosphonofluorescein readily enters living cells, showing excellent accumulation (>6x) and retention (>11x), resulting in a nearly 70-fold improvement in cellular brightness compared to 3-carboxyfluorescein. In a complementary fashion, the free acid form of 3-phosphonofluorescein does not cross cellular membranes, making it ideally suited for incorporation into a voltage-sensing scaffold. We develop a new synthetic route to functionalized 3-phosphonofluoresceins to enable the synthesis of phosphono-voltage sensitive fluorophores, or phosVF2.1.Cl. Phosphono-VF2.1.Cl shows excellent membrane localization, cellular brightness, and voltage sensitivity (26%  $\Delta F/F$  per 100 mV), rivaling that of sulfon-based VF dyes. In summary, we develop the first synthesis of 3-phosphonofluoresceins, characterize the spectroscopic properties of this new class of xanthene dyes, and utilize these insights to show the utility of 3-phosphonofluoresceins in intracellular imaging and membrane potential sensing.

## Phosphono-fluoresceins: synthesis and applications



## INTRODUCTION

Since the original synthesis of fluorescein in 1871,<sup>1</sup> this versatile molecule remains one of the most widely utilized fluorophores in biology, medicine, and chemical biology. Fluorescein labeled antibodies were the first immunofluorescent stains,<sup>2</sup> and reagents such as fluorescein isothiocyanate, or FITC, remain ubiquitous for the preparation of fluorescent biological conjugates.<sup>3</sup> One of the few fluorophores FDA-approved for use in humans, sodium fluorescein, has found clinical uses in ophthalmology<sup>4,5</sup> and more recently, neurosurgery.<sup>6</sup> A staple in the chemical biology community, countless fluorescein-derived probes and sensors have been reported over the years.<sup>7–9</sup> Design of such probes often take advantage of the ability to modulate fluorescence by substitution at the phenolic oxygen, control of spirocyclization, or changes in the rate of photoinduced electron transfer (PeT).<sup>8,10–12</sup> For example, appending BAPTA, a calcium chelator, to fluoresceins is a common strategy that makes use of PeT to modulate fluorescence and has enabled probing of intracellular calcium dynamics in neurons and brain tissue with high sensitivity and spatiotemporal resolution.<sup>13–15</sup>

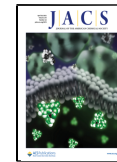
The wide utility of fluorescein and related xanthene dyes is due, in part, to their high brightness and wide range of colors

available with simple modifications to the terminal and bridgehead atoms of the xanthene fluorophore core. Replacement of the terminal oxygen atoms with substituted nitrogen results in another class of xanthene fluorophores: rhodamines. Spectral properties of rhodamines can be fine-tuned by varying the amine substitution,<sup>16</sup> for example, four-membered azetidines substantially improve brightness and photostability.<sup>17</sup> Replacement of the 10' oxygen atom with carbon,<sup>18,19</sup> silicon,<sup>20–23</sup> phosphorus,<sup>24–26</sup> or sulfur<sup>27</sup> red-shifts excitation and emission wavelengths, avoiding issues related to phototoxicity and autofluorescence and improving tissue penetration for *in vivo* imaging.

By comparison, substitution of the pendant carboxylate of fluoresceins has remained relatively underexplored. Substitution at the 3 position restricts free rotation of the *meso* ring, improving the fluorescence quantum yield.<sup>10</sup> The chemical

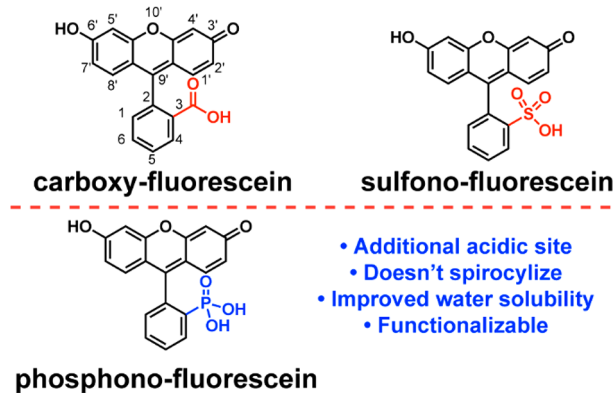
Received: January 29, 2021

Published: April 2, 2021



identity of the substitution at the 3 position can have profound effects on the properties of fluoresceins and related xanthenes. Fluoresceins spirocyclize at low pH or in low dielectric mediums to a nonfluorescent lactone, and this is often the basis for design of fluorogenic probes.<sup>12</sup> Substitution of the 3-carboxylate for hydroxymethyl, aminomethyl, or mercapto-methyl nucleophiles tunes the spirocyclization equilibrium of various rhodamines.<sup>28–30</sup> This led to the development of spontaneously blinking fluorophores for single molecule localization microscopy.<sup>28</sup> Sulfono-fluoresceins (Scheme 1),

### Scheme 1. Unique Properties of Phosphonofluorescein



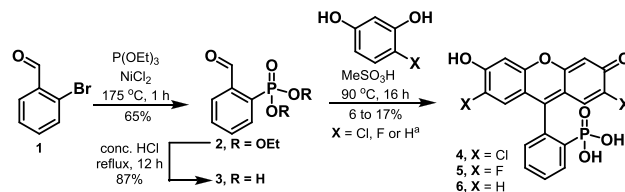
bearing a sulfonate at the 3 position, do not spirocyclize and have improved water solubility: properties that have been instrumental in the design of voltage sensitive fluorophores (VF dyes).<sup>31–34</sup>

While fluoresceins with acidic substituents at the 3 position have been ubiquitous in the literature for some time (3-sulfonofluorescein was reported a mere 13 years<sup>35</sup> after 3-carboxyfluorescein<sup>1</sup>), we were somewhat surprised to find no report describing 3-phosphonofluorescein, which possesses the biologically relevant acidic phosphonate group (Scheme 1). We were curious to explore this unreported class of fluoresceins and envisioned that 3-phosphonofluoresceins might have unique properties compared to 3-carboxyfluoresceins. For example, the two acidic sites on phosphonates, the first  $pK_a$  above sulfonic acid but below carboxylic acid, and a second  $pK_a$  near physiological pH,<sup>36</sup> might provide opportunities for functionalization. The persistent ionization of phosphonates at physiological pH might also enhance water solubility compared to 3-carboxyfluoresceins. Here, we report the first synthesis of 3-phosphonofluoresceins, characterize the spectral properties of this new class of fluorophore, and exploit the properties of 3-phosphonofluoresceins for two orthogonal live-cell imaging applications.

## RESULTS AND DISCUSSION

**Synthesis of 3-Phosphonofluoresceins.** Substituting the carboxylate functionality of fluoresceins poses an inherent synthetic challenge. Attempts to displace fluoride from 2-fluorobenzaldehyde with triethylphosphite, in a fashion analogous to the synthesis of 3-sulfonofluorescein precursors,<sup>32,37</sup> resulted in no reaction. However, Ni-mediated catalysis<sup>38,39</sup> enabled access to arylphosphonic ester 2 from 2-bromobenzaldehyde 1 in 65% yield (Scheme 2). A slight excess of triethyl phosphite is required due to undesired oxidation of the phosphite to the corresponding phosphate at elevated temperature. A weak nitrogen flow is also prudent to

### Scheme 2. Synthesis of Phosphonofluoresceins<sup>a</sup>



<sup>a</sup>For X = H the following conditions were used: H<sub>3</sub>PO<sub>4</sub> (85%), 130 °C, 2.5 days.

remove the generated ethyl bromide. This approach enabled facile access to up to 10 g quantities of 2 in one step from simple starting reagents. Hydrolysis to phosphonic acid 3 was performed in concentrated HCl under refluxing conditions to give the free acid in 87% yield. While the diethyl ester precursor (2) could be carried directly into the condensation with resorcinols to make 3-phosphonofluoresceins (with hydrolysis of diethylphosphonate occurring *in situ*), we observed improved yields and simpler purification when using free phosphonic acid (3). Condensation of 3 with the corresponding resorcinol in neat methanesulfonic acid gave dihalogenated phosphonofluoresceins 4 and 5. Nonhalogenated phosphonofluorescein (6) could also be prepared via this route, but cleaner conversion was observed with 85% phosphoric acid at the expense of a longer reaction time.

The purification of crude phosphonofluoresceins was difficult, owing to the high polarity of the water-soluble dyes. Careful trituration of the crude reaction isolate with mixtures of cold methanol/isopropanol or methanol/acetonitrile enabled isolation of pure dyes (Supporting Information (SI)). This approach negated the need for costly and low throughput reverse phase chromatographic techniques (such as HPLC) but came at the cost of reduced isolated yields, ranging from 6 to 17%. It is notable that this synthetic route provides similar yields to those observed with the analogous sulfonated derivatives (SI) and low yields/nontrivial purifications are commonly encountered with such reactions.

**Spectroscopic Characterization of 3-Phosphonofluorescein.** To examine the influence of phosphonate substitution on fluorescein, we evaluated the spectroscopic properties of 3-phosphonofluoresceins (4–6) compared to those of traditional 3-carboxy- and 3-sulfono- fluoresceins. In 0.1 M NaOH<sub>(aq)</sub> 2',7'-dichloro-3-phosphonofluorescein (pF.Cl, 4) absorbs at 498 nm and emits at 517 nm (Table 1, Figure S1a), demonstrating a very slight hypsochromic shift relative to 2',7'-dichloro-3-carboxyfluorescein (502 nm/523 nm, Table 1, Figure S1d).<sup>40</sup> The sulfone derivative, 2',7'-dichloro-3-sulfonofluorescein (sF.Cl), however, has a slight bathochromic shift and absorbs at 509 nm and emits at 526 nm (Table 1, Figure S1e). These small shifts are likely due to slight inductive differences from the *meso* ring. Since the *meso* ring and the xanthene are orthogonal to one another, there should be minimal ground state interactions between the two. As a result, the Stokes shift, extinction coefficients, and quantum yields show only minor variability across the series (Table 1). The photostability of 4 is similar to the 3-carboxy and 3-sulfono analogs (Figure S1g–i). One large change is the improved water solubility; pF.Cl (4) is almost twice as soluble as 2',7'-dichloro-3-carboxyfluorescein and slightly less soluble than sF.Cl (Table 1).

Table 1. Properties of Fluoresceins

Dye	3-substituent	$X^a$	$\lambda_{\text{max}} / \text{nm}^b$	$\lambda_{\text{em}} / \text{nm}^b$	$\epsilon / \text{M}^{-1}\text{cm}^{-1}{}^{b,c}$	$\Phi_{\text{fl}}^b$	Solubility <sup>d</sup>
fluorescein		-CO <sub>2</sub> H	-H	491	514	88000	0.92
2',7'-dichloro-3-carboxy-fluorescein		-CO <sub>2</sub> H	-Cl	502	523	86000	0.94
2',7'-dichloro-3-sulfonofluorescein (sF.Cl)		-SO <sub>3</sub> H	-Cl	509	526	87000	0.89
2',7'-dichloro-3-phosphonofluorescein (pF.Cl, 4)		-PO <sub>3</sub> H <sub>2</sub>	-Cl	498	517	88000	0.90
2',7'-difluoro-3-phosphonofluorescein (pF.F, 5)		-PO <sub>3</sub> H <sub>2</sub>	-F	488	508	84000	0.94
3-phosphonofluorescein (pF.H, 6)		-PO <sub>3</sub> H <sub>2</sub>	-H	487	508	75000	0.99

<sup>a</sup>See Scheme 2. <sup>b</sup>In 0.1 M NaOH<sub>(aq)</sub>. <sup>c</sup>At max absorption. <sup>d</sup>Measured in PBS relative to 2',7'-dichlorofluorescein

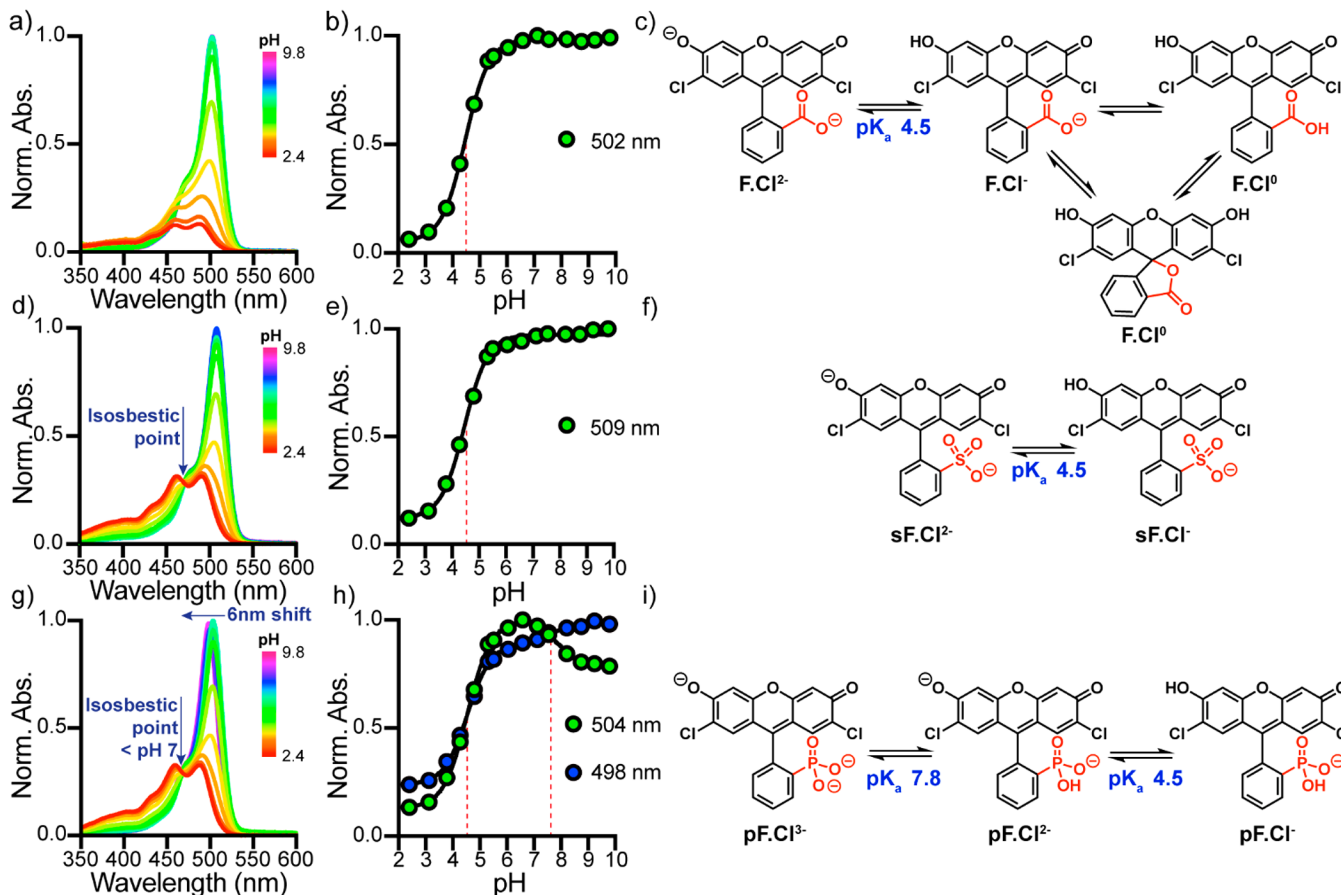


**Figure 1.** Spectroscopic characterization of the pH dependence of dichlorofluoresceins. Normalized absorbance spectra and corresponding plots of normalized absorbance vs pH at  $\lambda_{\text{max}}$  for carboxy- (a, b), sulfono- (d, e) and phosphono- (g, h) dichlorofluoresceins. Spectra were recorded in 10 mM buffered solutions (see SI) containing 150 mM NaCl from pH 2.4 (red) to 9.8 (magenta), and intermediate values of 3.1, 3.8, 4.3, 4.8, 5.3, 5.5, 6.1, 6.6, 7.1, 7.5, 8.2, 8.7, and 9.2 at a dye concentration of 2  $\mu\text{M}$ . Titration curves fit to sigmoidal dose response curves (solid black) enabled  $\text{p}K_{\text{a}}$  determination (dashed red). Error bars represent  $\pm \text{SEM}$  for  $n = 3$  independent determinations and if not visible are smaller than the marker. Summary of pH equilibria with determined  $\text{p}K_{\text{a}}$  values for carboxy- (c), sulfono- (f), and phosphono- (i) dichlorofluoresceins.

**pH Titration of 3-Phosphonofluoresceins.** Fluorescein can exist in cationic, neutral, anionic, or dianionic forms, making absorption and fluorescence of fluoresceins strongly pH dependent.<sup>41,42</sup> Halogenated (2',7'- dichloro or difluoro) fluoresceins have lower phenolic  $\text{p}K_{\text{a}}$  values than the corresponding unhalogenated fluorescein, making dichloro- and difluoro- fluoresceins less sensitive to biologically relevant pH fluctuations.<sup>40,43</sup> In order to assess the effect of *meso* substitution on the pH sensitivity, we titrated 3-carboxy, 3-sulfono, and 3-phosphono- dichlorofluoresceins from pH 2.3 to 9.8 (Figure 1a,d,g). Transition to the dianion can be monitored by measuring the increase in absorption at  $\lambda_{\text{max}}$  with respect to increasing pH (Figure 1b,e,h). The phenolic  $\text{p}K_{\text{a}}$  of all three dichlorofluoresceins is 4.5, suggesting substitution at

the 3 position has little effect on formation of the dianion (Figure 1c,f,i).

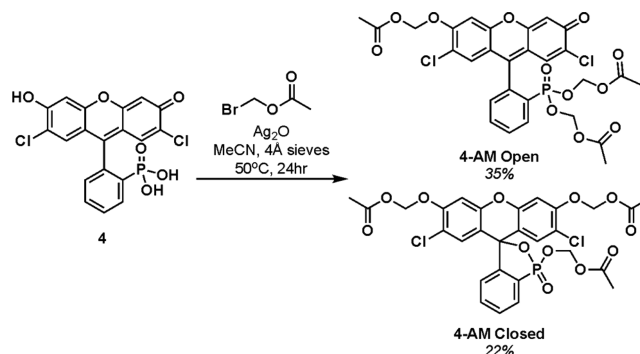
The  $\text{p}K_{\text{a}}$  values for nonhalogenated, 3-phosphonofluorescein (6,  $\text{p}K_{\text{a}} = 6.4$ ) and fluorinated 3-phosphonofluorescein (5,  $\text{p}K_{\text{a}} = 4.8$ ) also closely match the  $\text{p}K_{\text{a}}$  value of the analogous 3-carboxy analog (Figures S2 and S3).<sup>43</sup> Unique to 3-phosphonofluoresceins, after deprotonation to the dianion, a 5 nm hypsochromic shift is observed as pH continues to increase (Figure 1g, Figure S2a,c). This likely results from formation of a trianion (Figure 1i) due to the extra acidic site on the phosphonate, and quantification of this shift with 4 (pF.Cl) reveals a  $\text{p}K_{\text{a}}$  of 7.8—in the typical range of acidities for aryl phosphonic acids.<sup>34</sup>

**Cyclization Tendency of 3-Phosphonofluoresceins.** In the neutral form, carboxy fluoresceins spirocyclize to a colorless, nonfluorescent lactone (Figure 1c) whereas 3-sulfono-fluoresceins do not (Figure 1d–f). Both sulfono- and phosphono-dichlorofluoresceins have a clear isosbestic point between pH 2.3 and 6.8 (Figure 1d,g), resulting from the interconversion of the anionic quinoid and dianion. The same isosbestic point is not observed with 3-carboxy dichlorofluorescein, as absorption continuously decreases with pH due to spirocyclization to the neutral lactone at low pH (Figure 1a). The observation that carboxy-fluoresceins spirocyclize whereas sulfono- and phosphono-fluoresceins do not can be rationalized by the difference in  $pK_a$  values. The 3-substituents on the latter two are strongly acidic, with  $pK_a$  values lower than protonation of the xanthene to the cationic form (Figure S3c), and thus the neutral form favors an open zwitterion. The carboxylate, however, has a higher  $pK_a$ , so a significant portion of the neutral form exists as a closed lactone.<sup>41</sup> Fluorescein can also spirocyclize in low dielectric media and thus does not absorb light in the visible region (Figure S4a,b, red trace). In low dielectric media, both 3-phosphono- (Figure S4d–f) and 3-sulfono-fluoresceins (Figure S4c) possess absorbance profiles similar to the protonated xanthene in the open form. Moving from high to low dielectric, we observe an apparent increase in the  $pK_a$  of the phenolic oxygen but no tendency to spirocyclize into the colorless lactone.

**Cell Permeability and Retention.** Acetoxy methyl (AM) ethers are commonly employed to deliver anionic fluorophores and small molecules into cells.<sup>44</sup> The high  $pK_a$  (~13) of the formaldehyde hydrate leaving group provides chemical and hydrolytic stability, therefore AM ether hydrolysis relies on endogenous cellular esterases.<sup>45</sup> In the context of fluorescein, this uncaging process is fluorogenic; hydrolysis of the first AM ether releases the dye from its closed, colorless lactone form, and hydrolysis of the second AM ether provides the negatively charged phenolate responsible for strong fluorescence. This fluorogenicity has resulted in the widespread use of fluorescein AMs as cell viability reagents and has enabled the intracellular delivery of numerous fluorescein-derived probes.<sup>45,46</sup> Despite their widespread use, carboxy fluoresceins are rapidly effluxed out of cells, hindering the long-term imaging of live cells.<sup>47–49</sup> We considered whether the improved water solubility and lower  $pK_a$  of 3-phosphonofluoresceins would improve intracellular retention, since this charged group must be masked in some way in order to cross the lipid bilayer. While 3-sulfonofluoresceins also possess high water solubility and low  $pK_a$  values, sulfonic esters are potent electrophiles, making them inherently unstable and difficult to chemically mask for intracellular delivery.<sup>50</sup> Phosphonates are commonly masked with biologically labile protecting groups, such as AM esters, to deliver phosphonate containing molecules into cells.<sup>51–53</sup> This approach is commonly incorporated into the design of nucleotide (or nucleoside phosphate) prodrugs.<sup>54,55</sup>

Treatment of 3-carboxy-fluoresceins with bromomethyl acetate in the presence of Ag(I) in MeCN results predominantly in the closed, nonfluorescent, lactonized form with two phenolic AM ethers, although a small amount of the open AM ether/ester can be isolated.<sup>45</sup> Owing to the tendency to not spirocyclize, the opposite selectivity was observed with pF.Cl (4), where the open form (**4-AM open**) was the major product, and the cyclized form (**4-AM closed**) was the minor product (Scheme 3). In buffered saline (Hank's balanced salt solution, HBSS), **4-AM open** has absorption centered at 467

**Scheme 3. Synthesis of Phosphonofluorescein Acetoxy Methyl Esters and Ethers**



nm and emission profiles characteristic of a singly alkylated xanthene ether (Figure S5a,b). No hydrolysis was observed after several hours of incubation in HBSS at 37 °C (Figure S6). Incubation in strong base or in the presence of porcine liver esterase (PLE), however, resulted in a ~30x fold increase in fluorescence (Figure S6 and S5a,b), demonstrating effective release of the free dye and behaving in the same way as the analogous carboxy-fluorescein AM (Figure S5i,j). While the closed, 3-carboxy fluorescein AMs absorb no visible light in HBSS (Figures S5e–h), **4-AM closed**, with an absorption maximum at 443 nm, displays a spectrum (Figure S5c,d) similar to that of the cationic species observed at low pH (Figure S2b), suggesting the **4-AM closed** is in an open, zwitterionic form. Subsequent incubation of **4-AM closed** at 37 °C in HBSS for 2 h results in a loss of any visible absorption (Figure S5d) along with a decrease in  $m/z$  corresponding to loss of a single AM group (Figure S7). This suggests that in this form, the phosphono ester of **4-AM closed** is prone to facile hydrolysis (Figure S8). The  $^{31}\text{P}$  NMR chemical shift of **4-AM closed** is significantly downfield (30.3 ppm, Spectrum S23) relative to **4-AM open** (14.3 ppm, Spectrum S20), likely a result of increased electrophilicity, and thus confers decreased hydrolytic stability of **4-AM closed**.

Unsurprisingly, 4, which contains no AM esters, is cell impermeable and no uptake into HEK293T (HEK) cells was observed by fluorescence microscopy after 20 min of incubation (Figure 2a,d). The same is true for **4-AM closed**, suggesting the phosphonoester is rapidly hydrolyzed and the resulting negative charge precludes the ability to diffuse across the cell membrane (Figure 2b,e, Figure S8). The strong cellular fluorescence from cells treated with **4-AM open** indicates a high degree of cell permeability followed by fluorogenic uncaging (Figure 2c,f). Compared to 3-carboxyfluorescein AM derivatives, **4-AM open** has between 3.5 to 6-fold increase in cellular fluorescence intensity compared to FCl and F-AMs (both open and closed) at 500 nM in HEK cells (Figure 3a,d), enabling the phosphono derivative to be used at much lower concentrations. In fact, we saw reasonable fluorescence intensity at 100 nM concentrations, whereas carboxy fluoresceins are often loaded in the  $\mu\text{M}$  range.<sup>43</sup>

We postulated the increased cellular fluorescence intensity of 3-phosphonofluoresceins may result from improved cellular retention compared to 3-carboxyfluoresceins. Serial washing of cells loaded with FCl-AM (2',7'-dichloro-3-carboxyfluorescein) results in a dramatic loss of fluorescence, and after 3 washes, cellular fluorescence levels are 8% of original intensities (Figure 3b,c). Conversely, with **4-AM open**, cellular

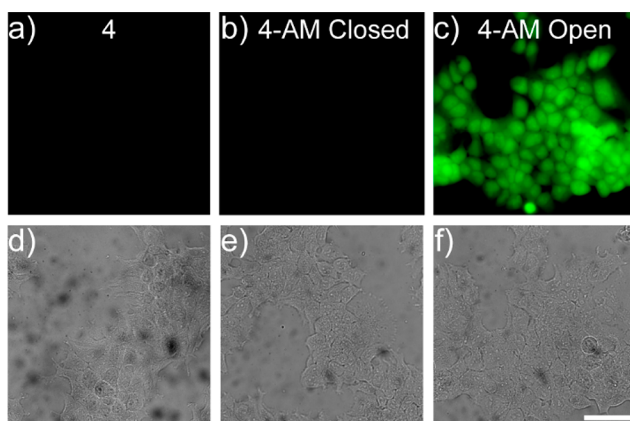


**Figure 2.** Cell permeability of phosphonofluoresceins. Widefield fluorescence (a–c) and DIC (d–f) images of HEK cells stained with 500 nM **4** (a,d), **4-AM closed** (b,e), and **4-AM open** (c,f) for 20 min at 37 °C. Cells were washed once with HBSS prior to imaging. Scale bar is 50  $\mu$ m.

fluorescence intensity levels remain at 89% of the original values, even after 3 washes (Figure 3b,c), thereby demonstrating an almost 70 fold increase in fluorescence intensity compared to cells stained with FCl-AM. The enhanced cellular retention of 3-phosphonofluoresceins expands the scope of use for prolonged imaging in living cells.

We then incubated HEK cells labeled with FCl-AM closed, 4-AM open, and calcein AM (a multiply carboxylated fluorescein derivative with excellent cellular retention)<sup>49,56</sup> in DMEM for up to 60 min prior to imaging. Carboxy fluorescein was rapidly effluxed, and no fluorescence was seen after the 0 min time point, whereas phosphonofluorescein appeared to efflux at a much slower rate, and almost half the intracellular fluorescence was retained after an hour (Figure S10b). Anionic transporters such as multidrug resistant-associated proteins (MRP) have been implicated in the efflux of fluorescein from cells, and MRP inhibitors such as MK-571 improve retention and accumulation of dyes.<sup>57–59</sup> Incubation of stained HEK cells in DMEM containing MK-571 (50  $\mu$ M) reduces the rate of dichlorofluorescein efflux after 15 min (Figure S10d); however, almost all cellular fluorescence was still lost after 60 min (Figure S10c). On the contrary, phosphonofluorescein efflux was almost completely inhibited by MK-571: no change in cellular fluorescence intensity was observed after 60 min incubation in the presence of MK-571 (Figure S10). One could imagine circumstances where moderate efflux of a fluorophore could prove beneficial, such as improving contrast when labeling intracellular structures. Phosphonofluorescein efflux can be readily inhibited with the addition of MK-571 for situations where efflux would be undesirable. Importantly, 3-phosphonofluorescein **4** shows very low cellular toxicity comparable that of calcein-AM,<sup>60</sup> a reagent used as a viability marker, when assayed using an MTT reduction assay (Figure S11).<sup>61</sup>

**Voltage Sensing with Phosphonofluoresceins.** The cellular uptake of 3-phosphonofluoresceins, like **4**, can be readily controlled by esterification of the 3-phosphonate, with the free phosphonic acid showing excellent exclusion from cells. Because of the tunable cellular permeability profile, high water solubility, and lack of spirocyclization, we hypothesized that 3-phosphonofluoresceins could be readily incorporated into a voltage-sensitive fluorophore (VoltageFluor) config-

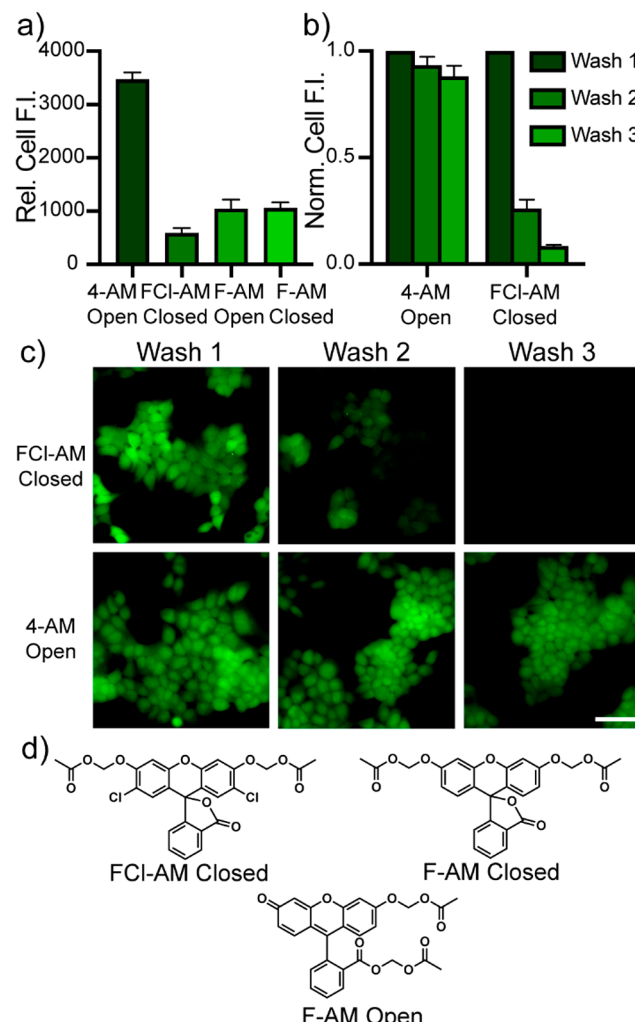
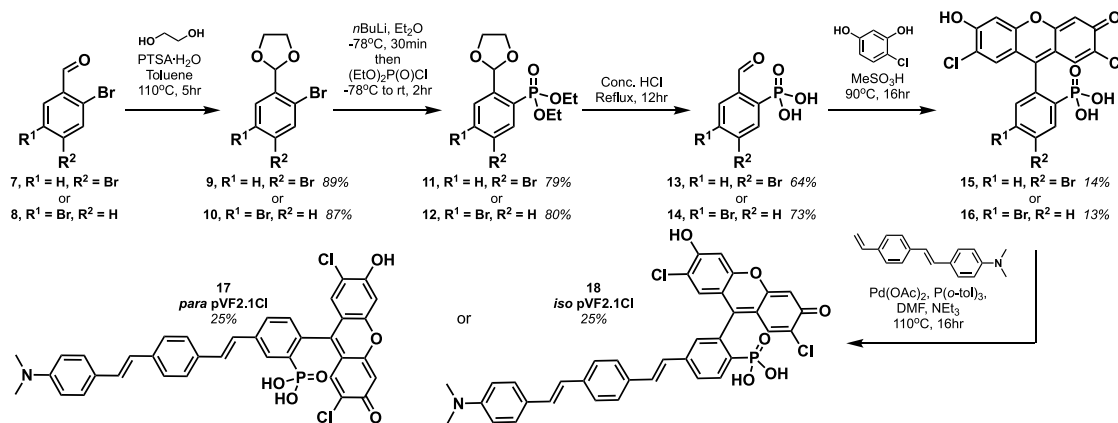


**Figure 3.** Cellular retention of fluoresceins. (a) Comparison of the relative brightness of fluorescein AMs in HEK cells. (b) normalized intensity and (c) fluorescence images of 4-AM Open and FCI-AM Closed loaded onto HEK cells at 500 nM in HBSS for 20 min. Cells were sequentially washed with fresh HBSS and changes in fluorescence intensity were measured by means of fluorescence microscopy. All dyes were loaded at 500 nM in HBSS for 20 min at 37 °C. Error bars in (a) and (b) are  $\pm$  SEM for  $n = 4$  coverslips. Scale bar is 50  $\mu$ m. (d) Chemical structures of carboxyfluorescein AMs.

uration, which employs voltage-sensitive photoinduced electron transfer (PeT) from a lipophilic, electron-rich, aniline-containing phenylene vinylene molecular wire into a fluorophore.<sup>34</sup> These VoltageFluors have primarily relied on 3-sulfonofluoresceins to prevent dye internalization and ensure proper orientation within the plasma membrane.<sup>32,62</sup>

The voltage-sensing molecular wire domains of VFs are typically installed via Heck coupling to fluoresceins, making use of a 5- or 6-halogen. Since we also require a halogen handle to install the phosphonate, we first protected 2,4- and 2,5-dibromo benzaldehydes (**7** and **8**) with ethylene glycol and used the corresponding acetals (**9** and **10**) to direct lithium-halogen exchange with *n*-butyllithium exclusively to the *ortho* position (Scheme 4). Slow addition of diethyl chlorophosphosphate and subsequent hydrolysis in concentrated acid yielded 4- and 5-bromo phosphono-benzaldehydes (**13** and **14**) which were condensed with 4-chlororesocinol to the corresponding 2',7'-dichloro-3-phosphonofluoresceins (**15** and **16**). The bromine

Scheme 4. Synthesis of Phosphono-VoltageFluors



functional group enabled Pd-catalyzed Heck coupling to a styrene molecular wire to produce *para* and *iso* phosVFs (**17** and **18**); however, only limited conversion occurred, and significant amounts of dehalogenated and unreacted dye were observed. We initially suspected this could be a result of the presence of the phosphonic acid functional group, but Pd-catalyzed cross coupling of phosphonate-containing precursor **13** and the same styrene resulted in a much greater 73% yield (SI **compound 19**). The desired phosVFs were, however, readily purified by reverse phase silica chromatography to give the desired products in 25% yield.

Both *para* and *iso* phosVFs possess absorbance and emission spectra nearly identical to those of pF.Cl (**4**), with the addition of an absorbance band at around 370 nm, corresponding to the aniline-containing molecular wire (Figure 4a, Figure S12). Both phosVF dyes localize to cellular membranes of HEK293T cells (Figure 4b, Figure S13) and are voltage sensitive (Figure 4c,d, Figure S14). Patch clamp electrophysiology coupled with fluorescence microscopy reveal that *para* phosVF2.1Cl has a voltage sensitivity of 26%  $\Delta F/F$  per 100 mV (Figure 4c,d), roughly the same sensitivity as the sulfonated analog, VF2.1Cl (24%).<sup>31,63</sup> The same trend was seen for *iso* phosVF2.1Cl and *iso* VF2.1Cl with  $\Delta F/F$  per 100 mV values of 11 and 9% respectively (Figure S14). No significant differences were observed in the relative brightness or signal-to-noise ratio when both *para* probes were loaded at 250 nM (Figure S13), suggesting that switching from a sulfonate to a phosphonate has a negligible effect on the orientation or ability to load into cellular membranes.

## CONCLUSIONS

In summary, we report the first synthesis of 3-phosphonofluoresceins, characterize the spectroscopic properties of this new class of fluorophore, and use 3-phosphonofluorescein in two orthogonal live-cell imaging applications. The new synthetic route to 3-phosphonofluorescein provides access to unhalogenated- and 2',7'-dihalogen-3-phosphonofluoresceins. 2',7'-Dichloro-3-phosphonofluorescein is more water-soluble than its 3-carboxy analog. In addition, 3-phosphonofluoresceins, unlike 3-carboxyfluoresceins, do not spirocyclize, thus rendering them cell-impermeant. Esterification of the phosphonic acid allows delivery of 3-phosphonofluoresceins to living cells, where they show an almost 70-fold increase in cellular brightness over carboxy fluorescein as a result of improved accumulation and retention. Finally, we adapt the synthesis of 3-phosphonofluoresceins to include 5- or 6-bromo

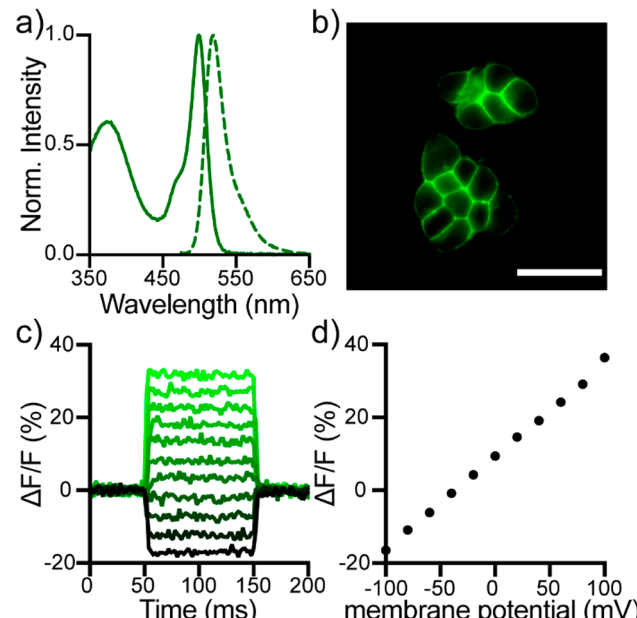


**Figure 4.** Cellular and *in vitro* characterization of phosphonated VoltageFluors. (a) Normalized absorbance (solid line) and fluorescence emission (dashed line) spectra of *para* phosVF2.1Cl (**17**) in 0.1 M NaOH<sub>(aq)</sub>. (b) HEK cells stained with 250 nM *para* phosVF2.1Cl (**17**). Scale bar is 40  $\mu$ m. (c) Plot of the fractional change in fluorescence of *para* phosVF2.1Cl (**17**) vs time for 100 ms hyper- and depolarizing steps ( $\pm 100$  mV in 20 mV increments) for single HEK cells under whole-cell voltage-clamp mode. (d) plot of  $\Delta F/F$  vs final membrane potential, revealing a voltage sensitivity of approximately 26% per 100 mV. Error bars are  $\pm$  SEM for  $n = 17$  cells. If not visible, error bars are smaller than the marker.

derivatives en route to voltage-sensitive 3-phosphonofluoresceins. These new phosVF dyes show excellent membrane staining and have voltage sensitivity rivaling the best fluorescein-based VF dyes.<sup>63</sup> We imagine that 3-phosphonofluoresceins will be of utility in long-term imaging applications that rely on a high degree of cellular retention and in voltage imaging applications. We envision that 3-phosphono substitution will yield additional opportunities in the context of xanthene dyes like rhodamines, and studies toward this end are underway in our lab.

## ■ ASSOCIATED CONTENT

### SI Supporting Information

The Supporting Information is available free of charge at <https://pubs.acs.org/doi/10.1021/jacs.1c01139>.

Experimental section, supporting figures, spectra, procedures, and analysis ([PDF](#))

## ■ AUTHOR INFORMATION

### Corresponding Author

Evan W. Miller — Departments of Chemistry, Molecular & Cell Biology, and Helen Wills Neuroscience Institute, University of California, Berkeley, California 94720, United States;  [orcid.org/0000-0002-6556-7679](https://orcid.org/0000-0002-6556-7679); Email: [evanwmiller@berkeley.edu](mailto:evanwmiller@berkeley.edu)

### Authors

Joshua L. Turnbull — Departments of Chemistry, University of California, Berkeley, California 94720, United States  
Brittany R. Benlian — Molecular & Cell Biology, University of California, Berkeley, California 94720, United States  
Ryan P. Golden — Departments of Chemistry, University of California, Berkeley, California 94720, United States

Complete contact information is available at:

<https://pubs.acs.org/10.1021/jacs.1c01139>

### Notes

The authors declare no competing financial interest.

## ■ ACKNOWLEDGMENTS

E.W.M. acknowledges generous support from the University of California, Berkeley, Klingenstein-Simons Fellowship in the Neuroscience, Camille Dreyfus Teacher-Scholar Fellowship, and the National Institute for General Medical Sciences (R35 GM119855). B.R.B. was supported, in part, by a training grant from NIGMS (T32GM666098).

## ■ REFERENCES

- (1) Baeyer, A. Ueber eine neue Klasse von Farbstoffen. *Ber. Dtsch. Chem. Ges.* **1871**, *4* (2), 555–558.
- (2) Coons, A. H.; Creech, H. J.; Jones, R. N.; Berliner, E. The Demonstration of Pneumococcal Antigen in Tissues by the Use of Fluorescent Antibody. *J. Immunol.* **1942**, *45* (3), 159.
- (3) Clark Brelje, T.; Wessendorf, M. W.; Sorenson, R. L., Chapter 5 - Multicolor Laser Scanning Confocal Immunofluorescence Microscopy: Practical Application and Limitations. In *Methods in Cell Biology*, Matsumoto, B., Ed. Academic Press: 2002; Vol. 70, pp 165–249e.
- (4) Wilson, S. A.; Last, A. Management of corneal abrasions. *American family physician* **2004**, *70* (1), 123–8.
- (5) Marmor, M. F.; Ravin, J. G. Fluorescein angiography: insight and serendipity a half century ago. *Arch. Ophthalmol. (Chicago, IL, U. S.)* **2011**, *129* (7), 943–8.
- (6) Cavallo, C.; De Laurentis, C.; Vetrano, I. G.; Falco, J.; Broggi, M.; Schiarioti, M.; Ferroli, P.; Acerbi, F. The utilization of fluorescein in brain tumor surgery: a systematic review. *Journal of neurosurgical sciences* **2018**, *62* (6), 690–703.
- (7) Johnson, I. D. *Molecular Probes Handbook: A Guide to Fluorescent Probes and Labeling Technologies*. Life Technologies Corporation: 2010; p 16.
- (8) Lavis, L. D.; Raines, R. T. Bright Building Blocks for Chemical Biology. *ACS Chem. Biol.* **2014**, *9* (4), 855–866.
- (9) Lavis, L. D. Teaching Old Dyes New Tricks: Biological Probes Built from Fluoresceins and Rhodamines. *Annu. Rev. Biochem.* **2017**, *86* (1), 825–843.
- (10) Urano, Y.; Kamiya, M.; Kanda, K.; Ueno, T.; Hirose, K.; Nagano, T. Evolution of Fluorescein as a Platform for Finely Tunable Fluorescence Probes. *J. Am. Chem. Soc.* **2005**, *127* (13), 4888–4894.
- (11) Miura, T.; Urano, Y.; Tanaka, K.; Nagano, T.; Ohkubo, K.; Fukuzumi, S. Rational Design Principle for Modulating Fluorescence Properties of Fluorescein-Based Probes by Photoinduced Electron Transfer. *J. Am. Chem. Soc.* **2003**, *125* (28), 8666–8671.
- (12) Grimm, J. B.; Heckman, L. M.; Lavis, L. D. The chemistry of small-molecule fluorogenic probes. *Progress in molecular biology and translational science* **2013**, *113*, 1–34.
- (13) Minta, A.; Kao, J. P.; Tsien, R. Y. Fluorescent indicators for cytosolic calcium based on rhodamine and fluorescein chromophores. *J. Biol. Chem.* **1989**, *264* (14), 8171–8.
- (14) Gee, K. R.; Brown, K. A.; Chen, W. N. U.; Bishop-Stewart, J.; Gray, D.; Johnson, I. Chemical and physiological characterization of fluo-4  $\text{Ca}^{2+}$ -indicator dyes. *Cell Calcium* **2000**, *27* (2), 97–106.
- (15) Roopa; Kumar, N.; Kumar, M.; Bhalla, V. Design and Applications of Small Molecular Probes for Calcium Detection. *Chem. - Asian J.* **2019**, *14* (24), 4493–4505.
- (16) Beija, M.; Afonso, C. A. M.; Martinho, J. M. G. Synthesis and applications of Rhodamine derivatives as fluorescent probes. *Chem. Soc. Rev.* **2009**, *38* (8), 2410–2433.
- (17) Grimm, J. B.; English, B. P.; Chen, J.; Slaughter, J. P.; Zhang, Z.; Revyakin, A.; Patel, R.; Macklin, J. J.; Normanno, D.; Singer, R. H.; Lionnet, T.; Lavis, L. D. A general method to improve fluorophores for live-cell and single-molecule microscopy. *Nat. Methods* **2015**, *12* (3), 244–50. 3 p following 250.
- (18) Grimm, J. B.; Sung, A. J.; Legant, W. R.; Hulamm, P.; Matlosz, S. M.; Betzig, E.; Lavis, L. D. Carbofluoresceins and Carborhodamines as Scaffolds for High-Contrast Fluorogenic Probes. *ACS Chem. Biol.* **2013**, *8* (6), 1303–1310.
- (19) Grimm, J. B.; Gruber, T. D.; Ortiz, G.; Brown, T. A.; Lavis, L. D. Virginia Orange: A Versatile, Red-Shifted Fluorescein Scaffold for Single- and Dual-Input Fluorogenic Probes. *Bioconjugate Chem.* **2016**, *27* (2), 474–480.
- (20) Fu, M.; Xiao, Y.; Qian, X.; Zhao, D.; Xu, Y. A design concept of long-wavelength fluorescent analogs of rhodamine dyes: replacement of oxygen with silicon atom. *Chem. Commun.* **2008**, No. 15, 1780–1782.
- (21) Egawa, T.; Koide, Y.; Hanaoka, K.; Komatsu, T.; Terai, T.; Nagano, T. Development of a fluorescein analogue, TokyoMagenta, as a novel scaffold for fluorescence probes in red region. *Chem. Commun.* **2011**, *47* (14), 4162–4164.
- (22) Hirabayashi, K.; Hanaoka, K.; Takayanagi, T.; Toki, Y.; Egawa, T.; Kamiya, M.; Komatsu, T.; Ueno, T.; Terai, T.; Yoshida, K.; Uchiyama, M.; Nagano, T.; Urano, Y. Analysis of Chemical Equilibrium of Silicon-Substituted Fluorescein and Its Application to Develop a Scaffold for Red Fluorescent Probes. *Anal. Chem.* **2015**, *87* (17), 9061–9069.
- (23) Grimm, J. B.; Brown, T. A.; Tkachuk, A. N.; Lavis, L. D. General Synthetic Method for Si-Fluoresceins and Si-Rhodamines. *ACS Cent. Sci.* **2017**, *3* (9), 975–985.
- (24) Fukazawa, A.; Usuba, J.; Adler, R. A.; Yamaguchi, S. Synthesis of seminaphtho-phospha-fluorescein dyes based on the consecutive arylation of arylidichlorophosphines. *Chem. Commun.* **2017**, *53* (61), 8565–8568.
- (25) Zhou, X.; Lai, R.; Beck, J. R.; Li, H.; Stains, C. I. Nebraska Red: a phosphinate-based near-infrared fluorophore scaffold for chemical biology applications. *Chem. Commun.* **2016**, *52* (83), 12290–12293.
- (26) Chai, X.; Cui, X.; Wang, B.; Yang, F.; Cai, Y.; Wu, Q.; Wang, T. Near-Infrared Phosphorus-Substituted Rhodamine with Emission Wavelength above 700 nm for Bioimaging. *Chem. - Eur. J.* **2015**, *21* (47), 16754–16758.
- (27) Liu, J.; Sun, Y.-Q.; Zhang, H.; Shi, H.; Shi, Y.; Guo, W. Sulfone-Rhodamines: A New Class of Near-Infrared Fluorescent Dyes for Bioimaging. *ACS Appl. Mater. Interfaces* **2016**, *8* (35), 22953–22962.
- (28) Uno, S.-n.; Kamiya, M.; Yoshihara, T.; Sugawara, K.; Okabe, K.; Tarhan, M. C.; Fujita, H.; Funatsu, T.; Okada, Y.; Tobita, S.; Urano, Y. A spontaneously blinking fluorophore based on intramolecular

spirocyclization for live-cell super-resolution imaging. *Nat. Chem.* **2014**, *6* (8), 681–689.

(29) Uno, S. N.; Kamiya, M.; Morozumi, A.; Urano, Y. A green-light-emitting, spontaneously blinking fluorophore based on intramolecular spirocyclization for dual-colour super-resolution imaging. *Chem. Commun. (Cambridge, U. K.)* **2018**, *S4* (1), 102–105.

(30) Zheng, Q.; Ayala, A. X.; Chung, I.; Weigel, A. V.; Ranjan, A.; Falco, N.; Grimm, J. B.; Tkachuk, A. N.; Wu, C.; Lippincott-Schwartz, J.; Singer, R. H.; Lavis, L. D. Rational Design of Fluorogenic and Spontaneously Blinking Labels for Super-Resolution Imaging. *ACS Cent. Sci.* **2019**, *5* (9), 1602–1613.

(31) Miller, E. W.; Lin, J. Y.; Frady, E. P.; Steinbach, P. A.; Kristan, W. B.; Tsien, R. Y. Optically monitoring voltage in neurons by photo-induced electron transfer through molecular wires. *Proc. Natl. Acad. Sci. U. S. A.* **2012**, *109* (6), 2114–2119.

(32) Kulkarni, R. U.; Yin, H.; Pourmandi, N.; James, F.; Adil, M. M.; Schaffer, D. V.; Wang, Y.; Miller, E. W. A Rationally Designed, General Strategy for Membrane Orientation of Photoinduced Electron Transfer-Based Voltage-Sensitive Dyes. *ACS Chem. Biol.* **2017**, *12* (2), 407–413.

(33) Ortiz, G.; Liu, P.; Naing, S. H. H.; Muller, V. R.; Miller, E. W. Synthesis of Sulfonated Carbofluorescins for Voltage Imaging. *J. Am. Chem. Soc.* **2019**, *141* (16), 6631–6638.

(34) Liu, P.; Miller, E. W. Electrophysiology, Unplugged: Imaging Membrane Potential with Fluorescent Indicators. *Acc. Chem. Res.* **2020**, *S3* (1), 11–19.

(35) Remsen, I. On a new class of compounds analogous to the phthaleins. *Am. Chem. J.* **1884**, *6*, 180–181.

(36) Franz, R. G. Comparisons of pKa and log P values of some carboxylic and phosphonic acids: Synthesis and measurement. *AAPS PharmSci* **2001**, *3* (2), 1.

(37) Kovi, R.; Nampalli, S.; Tharial, P. X. Process for preparation and purification of isosulfan blue. US20080281127A1, 2008.

(38) Tavs, P. Reaktion von Arylhalogeniden mit Trialkylphosphiten und Benzolphosphonigsäure-dialkylestern zu aromatischen Phosphonäureestern und Phosphinsäureestern unter Nickelsalzkatalyse. *Chem. Ber.* **1970**, *103* (8), 2428–2436.

(39) Balthazor, T. M.; Grabiak, R. C. Nickel-catalyzed Arbuzov reaction: mechanistic observations. *J. Org. Chem.* **1980**, *45* (26), 5425–5426.

(40) Leonhardt, H.; Gordon, L.; Livingston, R. Acid-base equilibria of fluorescein and 2',7'-dichlorofluorescein in their ground and fluorescent states. *J. Phys. Chem.* **1971**, *75* (2), 245–249.

(41) Martin, M. M.; Lindqvist, L. The pH dependence of fluorescein fluorescence. *J. Lumin.* **1975**, *10* (6), 381–390.

(42) Sjöback, R.; Nygren, J.; Kubista, M. Absorption and fluorescence properties of fluorescein. *Spectrochim. Acta, Part A* **1995**, *S1* (6), L7–L21.

(43) Sun, W.-C.; Gee, K. R.; Klaubert, D. H.; Haugland, R. P. Synthesis of Fluorinated Fluorescins. *J. Org. Chem.* **1997**, *62* (19), 6469–6475.

(44) Tsien, R. Y. A non-disruptive technique for loading calcium buffers and indicators into cells. *Nature* **1981**, *290* (5806), 527–528.

(45) Lavis, L. D.; Chao, T.-Y.; Raines, R. T. Synthesis and utility of fluorogenic acetoxyethyl ethers. *Chemical Science* **2011**, *2* (3), 521–530.

(46) Johnson, I. D. *Molecular Probes Handbook: A Guide to Fluorescent Probes and Labeling Technologies*. Life Technologies Corporation: 2010; p 835–6.

(47) Prosperi, E.; Croce, A. C.; Bottiroli, G.; Supino, R. Flow cytometric analysis of membrane permeability properties influencing intracellular accumulation and efflux of fluorescein. *Cytometry* **1986**, *7* (1), 70–5.

(48) Rotman, B.; Papermaster, B. W. Membrane properties of living mammalian cells as studied by enzymatic hydrolysis of fluorogenic esters. *Proc. Natl. Acad. Sci. U. S. A.* **1966**, *55* (1), 134–41.

(49) Izumi, S.; Urano, Y.; Hanaoka, K.; Terai, T.; Nagano, T. A Simple and Effective Strategy To Increase the Sensitivity of Fluorescence Probes in Living Cells. *J. Am. Chem. Soc.* **2009**, *131* (29), 10189–10200.

(50) Rusha, L.; Miller, S. C. Design and application of esterase-labile sulfonate protecting groups. *Chem. Commun.* **2011**, *47* (7), 2038–2040.

(51) Schultz, C.; Vajanaphanich, M.; Harootunian, A. T.; Sammak, P. J.; Barrett, K. E.; Tsien, R. Y. Acetoxyethyl esters of phosphates, enhancement of the permeability and potency of cAMP. *J. Biol. Chem.* **1993**, *268* (9), 6316–22.

(52) Li, W.; Schultz, C.; Llopis, J.; Tsien, R. Y. Membrane-permeant esters of inositol polyphosphates, chemical syntheses and biological applications. *Tetrahedron* **1997**, *53* (35), 12017–12040.

(53) Wiemer, A. J.; Wiemer, D. F., Prodrugs of Phosphonates and Phosphates: Crossing the Membrane Barrier. In *Phosphorus Chemistry I: Asymmetric Synthesis and Bioactive Compounds*, Montchamp, J.-L., Ed. Springer International Publishing: Cham, 2015; pp 115–160.

(54) Pradere, U.; Garnier-Amblard, E. C.; Coats, S. J.; Amblard, F.; Schinazi, R. F. Synthesis of Nucleoside Phosphate and Phosphonate Prodrugs. *Chem. Rev.* **2014**, *114* (18), 9154–9218.

(55) Schultz, C. Prodrugs of biologically active phosphate esters. *Bioorg. Med. Chem.* **2003**, *11* (6), 885–898.

(56) Diehl, H.; Ellingboe, J. L. Indicator for Titration of Calcium in Presence of Magnesium Using Disodium Dihydrogen Ethylenediamine Tetraacetate. *Anal. Chem.* **1956**, *28* (5), 882–884.

(57) Sun, H.; Johnson, D. R.; Finch, R. A.; Sartorelli, A. C.; Miller, D. W.; Elmquist, W. F. Transport of fluorescein in MDCKII-MRP1 transfected cells and mrp1-knockout mice. *Biochem. Biophys. Res. Commun.* **2001**, *284* (4), 863–869.

(58) Shugarts, S.; Benet, L. Z. The Role of Transporters in the Pharmacokinetics of Orally Administered Drugs. *Pharm. Res.* **2009**, *26* (9), 2039–2054.

(59) Gekeler, V.; Ise, W.; Sanders, K. H.; Ulrich, W. R.; Beck, J. The leukotriene LTD4 receptor antagonist MK571 specifically modulates MRP associated multidrug resistance. *Biochem. Biophys. Res. Commun.* **1995**, *208* (1), 345–52.

(60) Papadopoulos, N. G.; Dedoussis, G. V. Z.; Spanakos, G.; Gritzapis, A. D.; Baxevanis, C. N.; Papamichail, M. An improved fluorescence assay for the determination of lymphocyte-mediated cytotoxicity using flow cytometry. *J. Immunol. Methods* **1994**, *177* (1), 101–111.

(61) Kumar, P.; Nagarajan, A.; Uchil, P. D., Analysis of Cell Viability by the MTT Assay. *Cold Spring Harbor protocols* **2018**, *2018* (6). DOI: [10.1101/pdb.top096222](https://doi.org/10.1101/pdb.top096222)

(62) Deal, P. E.; Kulkarni, R. U.; Al-Abdullatif, S. H.; Miller, E. W. Isomerically Pure Tetramethylrhodamine Voltage Reporters. *J. Am. Chem. Soc.* **2016**, *138* (29), 9085–9088.

(63) Boggess, S. C.; Lazzari-Dean, J. R.; Raliski, B. K.; Mun, D. M.; Li, A. Y.; Turnbull, J. L.; Miller, E. W. Fluorescence lifetime predicts performance of voltage sensitive fluorophores in cardiomyocytes and neurons. *RSC Chemical Biology* **2021**, *2*, 248.